Energy and Buildings 66 (2013) 373–383

Contents lists available at ScienceDirect

Energy and Buildings

journal homepage: www.elsevier.com/locate/enbuild

Multi-criteria heatwave vulnerability assessment of residential wall systems

Jun Han*, Dong Chen, Xiaoming Wang

CSIRO Climate Adaptation Flagship and CSIRO Ecosystem Sciences, Commonwealth Scientific and Industrial Research Organisation (CSIRO), Highett, Victoria 3190, Australia

ARTICLE INFO

Article history:
Received 17 March 2013
Received in revised form 3 June 2013
Accepted 7 July 2013

Keywords:
Heatwave
Adaptation
Thermal performance
Overheating
Cooling load
Dynamic building simulation model
Finite difference approach

ABSTRACT

It is generally accepted that building external wall design affects its ability to protect occupants from weather extremes, such as heatwaves. However, there is no established methodology to assess this ability in assisting building designers to identify the most resilient design. This study aims at developing an analytical tool to examine wall heatwave vulnerability using dynamic thermal modelling and multi-criteria analysis. Optimum wall design for Melbourne was identified among eight selected residential walls based on various criteria, i.e. maximum air temperature (MAT), maximum air temperature difference (MATD), thermal discomfort proportion (TDP), statistical maximum air temperature (SMAT), and averaged night-time temperature (ANT). Using these criteria wall designs were ranked and ranking deviations among the criteria were analysed. Results showed that uninsulated brick veneer wall is the most vulnerable design, experiencing a maximum daytime room temperature of 31 °C and proportion in discomfort of 31.5% during heatwaves. While insulated cavity brick wall is found to be the most resilient design in most cases. The results indicate that using insulated cavity brick wall in Melbourne would significantly reduce summer overheating and thermal discomfort in non-air conditioned buildings in daytime period. It was found that no one criterion should be used for evaluating both daytime and night-time wall performance as ranking would be different between daytime and night-time periods. The decision procedure for design of a residential wall system may need to be reconsidered using the multi-criteria analysis, particularly under global warming.

1. Introduction

In the past decade, the number of extreme heatwaves has been on the rise globally, for example, the Shanghai in 2003 [1], the European in 2003 [2], the Greece in 2007 [3], the southern Australia in 2009 [4], and the U.S. in 2012 [5]. According to World Bank report 2012 [6], the global climate is warming, and its average temperature is anticipated to rise by 4 °C by the end of this century, without effective interventions. Such increases in the future climate are likely to lead to more frequent and longer heatwaves [7,8].

An intensifying heatwave event can have a significant social and economic impact on communities, especially on public health [9–11]. Public health problems, heat-related illness and deaths for example, might increase as a result of changing climate and increasing temperature. Research found that if outdoor ambient temperature increases beyond a particular threshold, so do mortality/morbidity rates [12].

As the main shelter of human beings, buildings play a vital role in protecting occupants from extreme environment and should be designed to cope with the warming climate and likely heatwave impacts. In this regard, we are now facing the challenges not only in designing low energy buildings to reduce greenhouse gas emissions for mitigating global warming, but also in maintaining required thermal comfort under changing climate, in particular, during extreme climate event. Current building codes, such as the Australian National Construction Code [13], set the criteria for regulating the energy efficiency of residential buildings. However, they consider little about the ability of current wall structures to buffer against extreme weather events and corresponding thermal stress to which occupants are exposed.

Consequently, in recent years, there is a growing interest in investigating the impact of climate change, possible adaptation and mitigation measures to reduce overheating risks. Various mitigation strategies were proposed and assessed, such as use of controls for blinds to reduce solar heat gain [14], natural ventilation [15–17], better construction material [18] and energy efficient building envelope [19], upgrading office IT equipment and light [20], double glazing [21]. The selection of building construction materials is one of the most important factors in designing a low energy and better

* Corresponding author. Tel.: +61 3 92526462; fax: +61 3 92526249.
E-mail addresses: bejunhan@gmail.com, jun.han@csiro.au (J. Han).

0378-7788/$ – see front matter © 2013 Elsevier B.V. All rights reserved.
http://dx.doi.org/10.1016/j.enbuild.2013.07.015

Nomenclature

A	area (m^2)
a	constant (–)
b	constant (–)
Bi	Biot number (–)
Cp	specific heat capacity (J/kg K)
C_t	turbulent natural convection constant (–)
Fo	Fourier number (–)
G_T	intensity of solar radiation on wall (W/m^2)
g	acceleration of gravity (m/s^2)
H	height of the air gap (m)
h	convective heat transfer coefficient (W/m^2 K)
$\bar{h}$	average heat transfer coefficient (W/m^2 K)
k	thermal conductivity (W/m K)
L	width of the air gap (m)
$\overline{Nu_L}$	average Nusselt number (–)
n	number of material or space surface (–)
Pr	Prandtl number (–)
Ra_L	Rayleigh number (–)
$SHGC$	solar heat gain coefficient (–)
T	temperature (°C)
t	time (s)
U_{win}	heat loss coefficient (W/m^2 K)
V	volume of space (m^3)
V_0	wind velocity (m/s)
x	coordinate as defined (–)

Greek symbols

α	thermal diffusivity (m^2/s)
β	volumetric thermal expansion coefficient (K^{-1})
ρ	density (kg/m^3)
ν	kinematic viscosity (m^2/s)
ε	absorptivity (–)

Subscripts

air	room air or air in the gap of wall
c	refers to cold wall
D	thickness of solid wall
d	thickness of air cavity
e	environment
g	air gap
h	refers to hot wall
i	inner surface of wall
in	inside or indoor
j	number of material
max	maximum
N	number of node
o	outside
r	roof
wf	wall surface and fluid in the air gap of the wall
win	window
*w*1	left wall surface of the air gap in the cavity wall
*w*2	right wall surface of the air gap in the cavity wall

thermal comfort building in response to large diurnal temperature swings [22]. Porritt et al. [23] claimed that external wall insulation and measures to reduce solar heat gain are the most effective interventions to reduce overheating as a result of heatwaves. Internal wall insulation seems less effective and could even increase overheating in some cases [24]. In addition, building form is another important factor in designing a comfort building to modify or filter climate extremes. An integrated design of building construction material and building form as a total system is a sustainable way to achieve optimum comfort and energy savings without heavily depending on mechanical cooling systems. This passive building design strategy does not have a high initial cost, while it provides an effective solution to mitigate heatwave.

In addition to the effect of climate change, the urban heat island (UHI) phenomenon as another contributing factor to overheating in buildings cannot be neglected. Indoor temperature and its related overheating risk in urban buildings are likely to be exacerbated in the future as a result of the combined effect of UHI effects and climate change [25]. According to Coutts [39], a mean maximum UHI intensity of 3–4 °C at 2 a.m. in January in Melbourne was predicted using an urban canopy model software. Oikonomou et al. [26] compared the relative importance of UHI and the thermal quality of dwellings for overheating in London. Their study indicates that the thermal characteristics of a dwelling have a greater effect on indoor temperatures during the 'hot' period than the UHI itself. The effects of built form and other dwelling characteristics appear to be more important determinants of indoor thermal performance.

The relationship between thermal comfort and building design has been well recognised and investigated among building professionals in the past. Various overheating assessment criteria were adopted and applied based on different purposes. A simple approach, such as static thresholds of comfort, is sometimes used to define when a building might be too warm [27]. Another criterion, the adaptive comfort criterion, takes consideration of adaptive approach to thermal comfort. Upper limits for temperatures in building with and without heating and cooling are suggested in terms of running mean of the outdoor temperature [28]. Nicol et al. [29] suggested that criteria for building overheating can be defined as achieving a specified Potential Discomfort Index (PDI) and also described an approach to predict the magnitude or frequency of overheating in buildings. Wright et al. [30] measured the internal temperatures in four dwellings in Manchester and five dwellings in London, of diverse ages, sizes and constructions during the August 2003 heatwaves. Resultant statistics and various comfort metrics indicated a high level of discomfort in most dwellings, particularly in London. Sakka et al. [31] investigated indoor thermal characteristics in 50 free-running low income houses during the extremely hot summer of 2007 in Athens, Greece. Very high indoor temperatures, up to 40 °C, were observed.

The above literature review indicates that warming climate due to climate change and UHI will increase the risk of overheating. However, few studies have been conducted to assess the heat vulnerability of residential walls in order to identify optimal building design which can result in reduced energy consumption during extreme heatwave event while maintaining thermal comfort requirement at the same time. The current study is to examine the vulnerability of selected Australian residential walls to heatwave in Melbourne using dynamic thermal modelling. Numerical simulations of the periodic heat transfer through various walls were carried out first. Then the dynamic thermal performance of wall systems and their resulted room air temperature were compared and analysed in terms of various assessment criteria in order to identify effective wall designs to accommodate heatwaves in Melbourne.

2. Dynamic thermal modelling

2.1. Heat transfer in solid walls

The purpose of the study is to examine the vulnerability of various residential walls to heatwaves. Eight different wall structures selected from Australian residential wall catalogue were studied. Traditional weatherboard wall is not included in the present study, as it is now not commonly used for new residential building

Table 1
Construction details of residential walls.

Number	Wall construction details	Wall name
A	Brickwork (110 mm)–air gap (40 mm)–polystyrene expanded (39 mm)–brickwork (110 mm)–plasterboard (10 mm)	'CavBrInP'
B	Aerated autoclaved concrete block (200 mm)–plasterboard (10 mm)	'ACC100'
C	Brickwork (110 mm)–air gap (40 mm)–brickwork (110 mm)–plasterboard (10 mm)	'CavBrUninP'
D	Hollow concrete block work (190 mm)–polystyrene expanded (39 mm)–plasterboard (10 mm)	'CTT190InP'
E	Concrete (100 mm)-plasterboard (10 mm)	'CTT100P'
F	Concrete (150 mm)–plasterboard (10 mm)	'CTT150P'
G	Brickwork (110 mm)–air gap (40 mm)–plasterboard (10 mm)	'BrVP'
H	Timber chardwood (40 mm)-air gap (40 mm)-brickwork (110 mm)-plasterboard (10 mm)	'CavWoP'

Table 2
Thermal properties of building construction materials.

Material	Density (kg/m^3)	Thermal conductivity (W/m K)	Specific heat capacity (J/kg K)
Aerated autoclaved concrete block	600	0.18	1000
Brickwork	1700	0.84	800
Concrete medium weight	1400	0.51	1000
Polyurethane	30	0.025	1400
Plasterboard	950	0.16	840

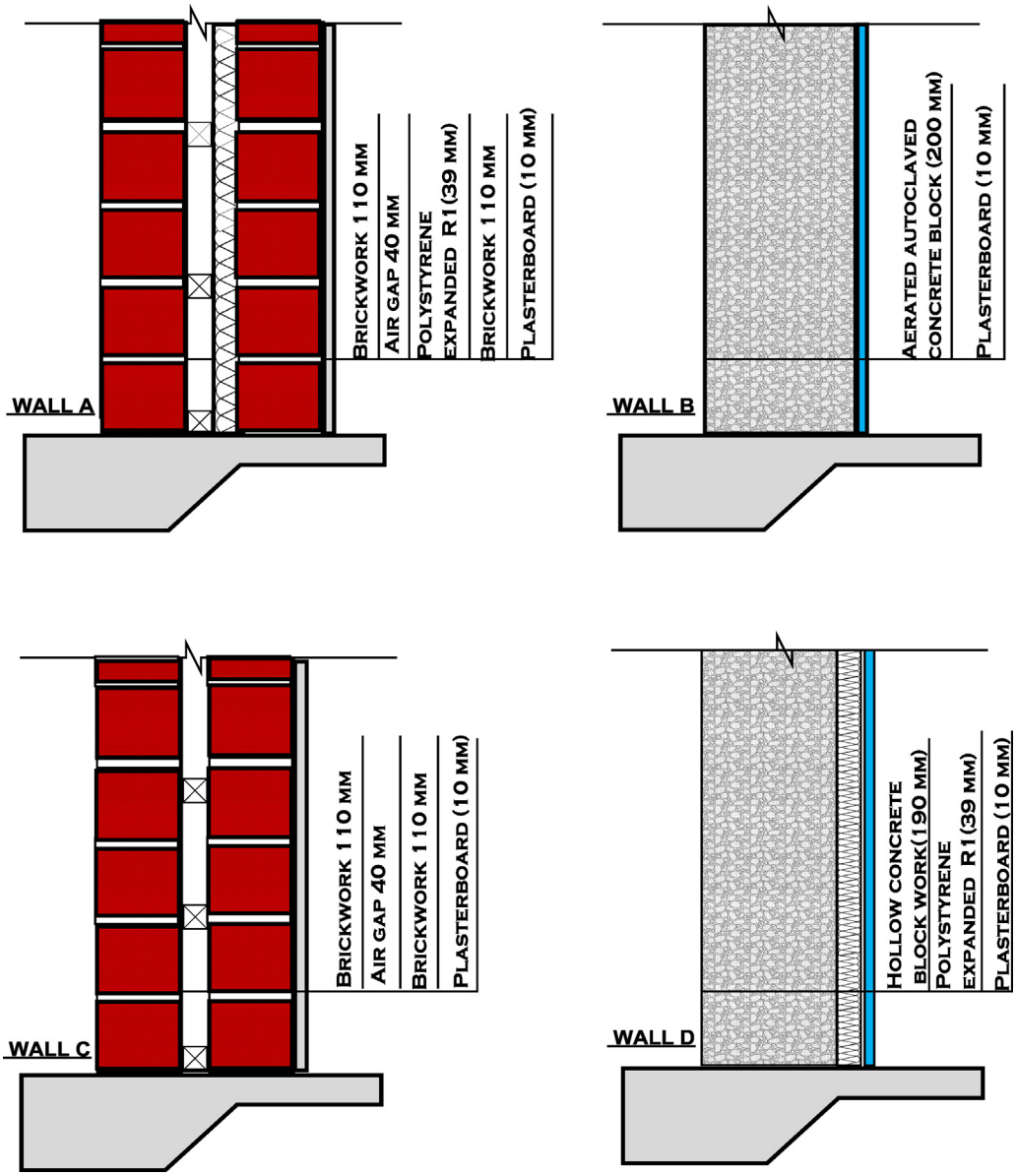

Fig. 1. Cross section schematics of eight different Australian residential walls.

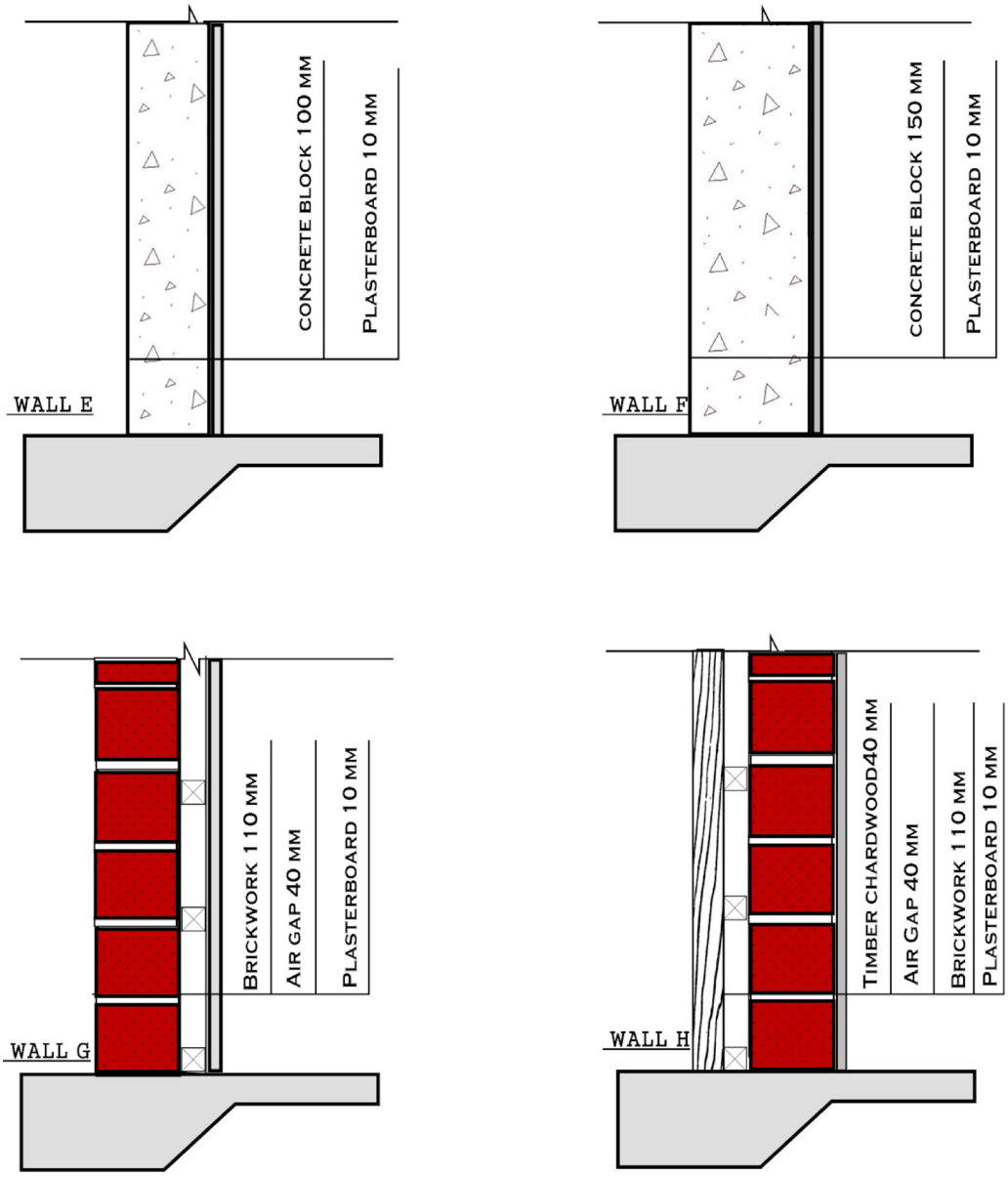

Fig. 1. (*Continued*).

construction in Melbourne. The schematics of the walls are shown in Fig. 1, and their thermal properties are listed in Tables 1 and 2.

For the composite wall system considering various layer thicknesses and thermal properties, a one-dimensional transient heat transfer equation without internal heat generation was employed. The outer surface of the wall is subjected to convection heat transfer, solar radiation, and long-wave radiation heat exchanges, while the inner surface is exposed to the indoor space of a single zone detached house as shown in Fig. 2. The governing partial differential equation (PDE) of the conductive heat transfer through the composite wall is described as:

$$\frac{\partial T_j(x,t)}{\partial t} = \frac{k_j}{\rho_j c_j}\frac{\partial^2 T_j(x,t)}{\partial x^2}, \quad j = 1, 2, \ldots, n \tag{1}$$

where x and t are the space and time coordinates, respectively; T_j is the temperature of the jth layer, °C; ρ_j, c_j, k_j are the density, kg/m^3, the specific heat, J/kg K, and the thermal conductivity of the jth layer material, W/m K, respectively; and n is the total number of material layers in a wall.

The adjacent layers are assumed to be in good thermal contact, and hence the interface resistance is negligible. The thermal conduction of the adjacent layers is expressed by:

$$T_j(x,t) = T_{j+1}(x,t), \quad j = 1, 2, \ldots, n-1 \tag{2}$$

$$k_j\frac{\partial T_j(x,t)}{\partial x} = k_{j+1}\frac{\partial T_{j+1}(x,t)}{\partial x}, \quad j = 1, 2, \ldots, n-1 \tag{3}$$

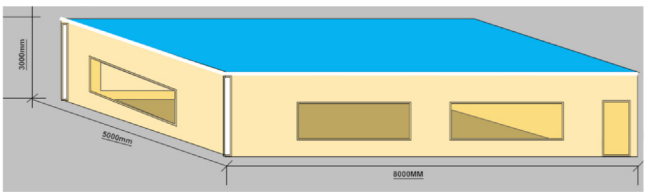

Fig. 2. Geometries of a single zone detached house.

Table 3
MoWiTT model constants.

Wind direction	C_t (W/m^2 K$^{4/3}$)	a (W/m^2 K(m/s)^b)	b (–)
Windward	0.84	2.38	0.89
Leeward	0.84	2.86	0.617

The initial temperature distribution across the wall is assumed to be uniform and is expressed as follows:

$$T_j(x, 0) = T_0 \tag{4}$$

The boundary conditions at the inner surface of the wall are given as follows:

$$-k_1 \frac{\partial T(x,t)}{\partial x}\bigg|_{x=0} = h_i(T_{in} - T_{x=0}) \tag{5}$$

where h_i is the convection heat transfer coefficient, W/m^2 K; from the ASHRAE handbook of fundamentals [32]: h_i = 9.26W/m^2 K for upward direction of heat flow, and h_i = 6.13 W/m^2 K for downward direction of heat flow, T_{in} is the room temperature, °C.

The boundary conditions at the outer surface are:

$$-k_n \frac{\partial T(x,t)}{\partial x}\bigg|_{x=D} = h_0(T_{x=D} - T_e) \tag{6}$$

Here, T_e, the sol–air temperature is calculated based on the ambient temperature, solar radiation and heat transfer coefficient [33].

$$T_e = T_0 + \frac{\varepsilon G_T}{h_0} \tag{7}$$

where ε is the solar absorptivity of the outer surface of the wall; G_T is the total intensity of solar radiation incident upon the outer surface of the wall, which is calculated according to sun position and follows the procedure in author's previous work [34], W/m^2; $T_{x=D}$ is the temperature of the outer surface of the wall, °C; T_0 is the ambient temperature, °C. The convective heat transfer coefficient of the outer surface, h_0, is dependent on the outdoor air conditions, such as air velocity and its direction, and the temperature difference between the wall outer surface and the ambient air. According to the MoWiTT model [35], the coefficient can be determined as follows:

$$h_0 = \sqrt{[C_t(\Delta T)^{1/3}]^2 + [aV_0^b]^2} \tag{8}$$

where C_t is the turbulent natural convection constant; ΔT is the temperature difference between the outer surface and outside air; a and b are constants; V_0 is wind speed at standard conditions, m/s. The values of the coefficients and constants for the MoWiTT model are summarised in Table 3.

2.2. Heat transfer in the air cavity of the wall

For the air cavity in a wall:

$$\rho V c \frac{dT_\infty}{dt} = h_{wf}A_g(T_{w1} - T_\infty) + h_{wf}A_g(T_{w2} - T_\infty) \tag{9}$$

where T_∞ is temperature in the air cavity, °C; ρ is the density of the air in the cavity, kg/m^3; V is air volume in the cavity, m^3; c is specific heat capacity of air, J/kg K. A_g is wall surface area; h_{wf} is overall heat transfer coefficient which will be further discussed in Section 2.4, T_{w1} andT_{w2} are left and right side wall surface temperatures, respectively, °C. They are calculated by Eqs. (1), (10) and (11).

The surface energy balances at the two surfaces of the air cavity in the wall are:

$$-k\frac{\partial T(x,t)}{\partial x}\bigg|_{x=D} = h_{wf}(T_{w1} - T_\infty) \tag{10}$$

$$-k\frac{\partial T(x,t)}{\partial x}\bigg|_{x=D+d} = h_{wf}(T_\infty - T_{w2}) \tag{11}$$

where d denotes the thickness of the air in the wall.

2.3. Heat balance of the room air

An enclosed single-zone building of internal volume V is considered with various external wall designs as shown in Fig. 2. The air in the building is assumed to be well-mixed with a uniform air temperature. Internal heat gain, air exchange and latent heat load are not considered for ease of wall performance comparison. Adiabatic boundary conditions are applied to the floor. The heat balance of the room air is described as:

$$\rho V c\frac{dT_{in}}{dt} = \sum_{i=1}^{n} h_{wf}A_{w,i}(T_{w,i} - T_{in}) + h_r A_r(T_r - T_{in}) + \sum_{i=1}^{n} U_{win}A_{win,i}(T_{out} - T_{in}) + \sum_{i=1}^{n} G_{T,i}A_{win,i}SHGC \tag{12}$$

where ρ is the density of the air in the room, kg/m^3; V is the volume of the room; c is specific heat capacity of air T_{in} is room air temperature, °C; h_{wf} is overall heat transfer coefficient between wall and room air, W/m^2 K; $A_{W,i}$ is the surface area of the ith wall, m^2; $T_{W,i}$ is the surface temperature of the ith wall, °C; h_r is convective heat transfer coefficient of the roof, W/m^2 K; T_r is the interior surface temperature of the roof, °C; U_{win} is the overall heat loss coefficient of the windows, U_{win} = 4.2 W/m^2 K, [32]; $A_{win,i}$ is the surface area of the ith window, m^2; T_{out} is outdoor ambient temperature, °C; $G_{T,i}$ is solar radiation striking the vertical surface, W/m^2; $SHGC$ is solar heat gain coefficient of a double glazed window assumed at $SHGC$ = 0.71 [36].

2.4. Heat transfer coefficients

The convective heat transfer coefficients in the air gap of the cavity wall types, such as 'wall A, C, G, H' were determined through a set of existing correlations in the literature. The following correlations proposed by Catton [37] have been used:

$$\overline{Nu_L} = 0.22\left(\frac{Pr}{0.2+Pr}Ra_L\right)^{0.28}\left(\frac{H}{L}\right)^{-1/4}, \quad \text{for} \begin{bmatrix} 2 < \frac{H}{L} < 10 \\ Pr < 10^5 \\ Ra_L < 10^{10} \end{bmatrix} \tag{13}$$

$$\overline{Nu_L} = 0.18\left(\frac{Pr}{0.2+Pr}Ra_L\right)^{0.29}, \quad \text{for} \begin{bmatrix} 1 < \frac{H}{L} < 2 \\ 10^{-3} < Pr < 10^5 \\ 10^3 < (Ra_L Pr)/(0.2+Pr) \end{bmatrix} \tag{14}$$

The Rayleigh number Ra_L is determined by the following formula:

$$Ra_L = \frac{g\beta(T_{w1} - T_{w2})L^3}{\alpha\nu} \tag{15}$$

Convection coefficients for the vertical cavity heated from one side may be obtained from the following corrections. All properties are evaluated at the mean temperature, $(T_{w1} + T_{w2})/2$.

$$\overline{Nu_L} = \frac{\overline{h}L}{k} \tag{16}$$

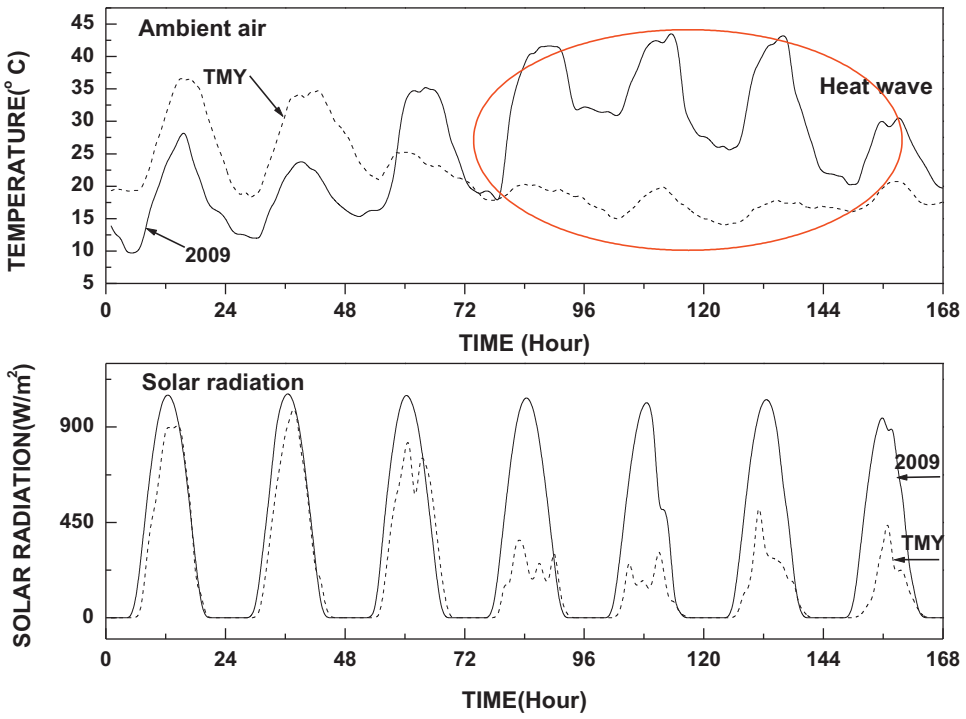

Fig. 3. Ambient air temperature and global solar radiation from TMY and 2009 (25th–31st January 2009) weather data of Melbourne showing record breaking heatwave by the red circle.

where $\overline{Nu_L}$ is average Nusselt number which is the ratio of convective to conductive heat transfer; Ra_L is Rayleigh number; Pr is Prandtl number; H is height of air gap, m; L is the thickness of air gap, m; g is acceleration of gravity, $g = 9.8\ m/s^2$; β is volumetric thermal expansion coefficient, K^{-1}; T_{w1} and T_{w2} are left and right side wall surface temperatures, °C; ν is kinematic viscosity, m^2/s; α is thermal diffusivity, m^2/s; $\bar{h}$ is average heat transfer coefficient, $W/m^2\ K$.

3. Numerical solution procedure

The transient heat transfer equations as shown in Section 2 are solved numerically by explicit finite difference approach. A computer code using Fortran 90 compiler has been developed for the solution of the above equations. The following lists finite difference equations for various nodes including the interior nodes, boundary nodes, interface face nodes between two layers of different materials.

3.1. Finite difference formulations

A dynamic model is introduced for analysing the transient heat transfer through the walls, which was solved by the control volume finite-difference method employing an explicit scheme.

The exterior and interior boundary nodes:

$$T_1^{n+1} = 2Fo(BiT_e^n + (1/2Fo - 1 - Bi)T_1^n + T_2^n) \quad (17)$$

$$T_N^{n+1} = 2Fo(T_{N-1}^n + (1/2Fo - 1 - Bi)T_N^n + BiT_{in}^n) \quad (18)$$

The interior nodes within same material:

$$T_i^{n+1} = Fo(T_{i-1}^n + (1/Fo - 2)T_i^n + T_{i+1}^n) \quad (19)$$

The interface nodes between two different materials:

$$T_i^{n+1} = 2Fo_jT_{i-1}^n + (1 - 2Fo_j - 2Fo_{j+1})T_i^n + 2Fo_{j+1}T_{i+1}^n \quad (20)$$

The air in the cavity of the wall:

$$T_{air}^{n+1} = \frac{\Delta t}{\rho Vc}\left(h_{wf}A_g(T_{w1}^n - T_{air}^n) + h_{wf}A_g(T_{w2}^n - T_{air}^n)\right) + T_{air}^n \quad (21)$$

The air in the room:

$$T_{in}^{n+1} = \frac{\Delta t}{\rho Vc}\left(\sum_{i=1}^{n} h_{wf}A_{w,i}(T_{w,i}^n - T_{in}^n) + h_rA_r(T_r^n - T_{in}^n) + \sum_{i=1}^{n} U_{win}A_{win,i}(T_{out}^n - T_{in}^n) + \sum_{i=1}^{n} G_{T,i}^n A_{win,i}SHGC\right) + T_{in}^n \quad (22)$$

where:

$$Bi = \frac{h_0\Delta x}{k} = \text{Biot number} \quad (23)$$

$$Fo_j = \frac{k_j\Delta t/\Delta x_j}{\rho_jc_j\Delta x_j + \rho_{j+1}c_{j+1}\Delta x_{j+1}} = \text{Fourier number for material } j \quad (24)$$

Here, the Biot number is a ratio of the heat transfer resistance inside of and at the surface of a body in interest.

3.2. Stability requirements

For stability consideration of the explicit scheme, the stability requirements for the internal, boundary and interface nodes are listed as follows:

For the internal node:

$$-(2 - 1/Fo) \geq 0 \text{ or } Fo \leq \tfrac{1}{2} \quad (25)$$

For the boundary nodes:

$$-(1 + Bi - 1/2Fo) \geq 0 \text{ or } Fo \leq \frac{1}{2(1 + Bi)} \quad (26)$$

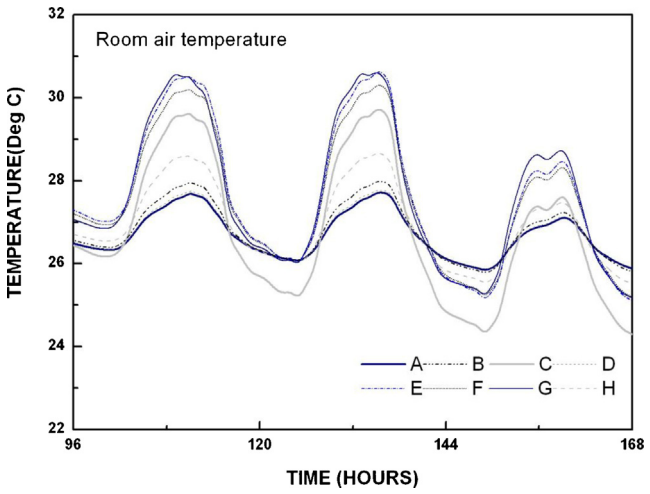

Fig. 4. Room air temperature comparisons of various residential walls for three consecutive days (28th–30th January 2009).

For the interface nodes between the composite layers of different materials:

$$-(2Fo_j + 2Fo_{j+1} - 1) \geq 0 \text{ or } (Fo_j + Fo_{j+1}) \leq \frac{1}{2} \quad (27)$$

4. Results and analysis

4.1. Weather data

The recorded weather data of Melbourne in 2009 were used as the model input to assess and predict the resilience capability of different residential walls to the heatwave. For comparison purposes, Typical Meteorological Year (TMY) data file of Melbourne, which is commonly used for building energy simulation, was also employed for model input. The model output includes the internal wall surface temperatures and hourly indoor temperature in response to the outdoor weather conditions.

Fig. 3 shows the ambient air temperature and global solar radiation on 25th–31st January 2009. During the extremely hot period, Melbourne has experienced a record prolonged heatwave, with three days over 43 °C and its CBD area reached 44.2 °C, when the latest heatwave and 'Black Saturday' hit Victoria on 7th February 2009. The circle in Fig. 3 illustrates this record breaking heatwave period.

4.2. Averaged maximum air temperature during heatwave

The room air temperatures in the building with different wall systems in the heatwave period were predicted using the dynamic model described in Sections 2 and 3. Fig. 4 compares the room air temperatures for the eight wall systems. The averaged maximum air temperatures, which are defined as the means of the daily maximum air temperatures during the heatwave period for the eight wall systems are compared in Table 4. It also lists wall relative heatwave vulnerability rankings in terms of the Averaged Maximum Air Temperature (AMAT) index, the higher the vulnerability ranking, the more vulnerable the wall system. It was found that 'wall A' shows a better thermal performance with the lowest AMAT for three consecutive days from 28th to 30th January 2009. 'Wall G' is more sensitive to external weather conditions especially the ambient temperature fluctuation.

Different from previous work in the literature using maximum air temperature in an office building as an indicator for overheating assessment [28], AMAT index uses the mean peak daily temperature during the heatwave period. AMAT provides a straightforward way of comparing the peak daytime temperatures inside a building by using different wall systems. However, it doesn't consider the night-time temperature at sleeping time. This weakness makes it difficult to assess thermal environment in particular when walls with high thermal mass release heat during night-time period. The released heat intends to increase the internal air temperature at night.

4.3. Maximum air temperature difference during heatwave

Maximum Air Temperature Difference (MATD) index is defined as the maximum difference in the room air temperatures predicted for the same period with TMY weather data and those during the heatwave period. Table 4 lists the MATD for the eight wall systems and their relative heatwave vulnerability rankings. In terms of MATD, 'wall A' performs the best with MATD at 1.58 °C. 'wall G' is more vulnerable to the outdoor climate change with MATD reaching about 4.29 °C as shown in Fig. 5. The maximum room air temperature during the heatwave period for 'wall A' is found to be 27.72 °C, while 30.65 °C for 'wall G'. MATD services as an indicator of internal temperature difference between two weather conditions, i.e., normal and extremes. Vulnerable design thus could be clearly identified by using this index. It provides useful reference for building energy budget planning considering the effect of weather extremes. However, similar to AMAT, MATD is an index closely related to the maximum daytime room air temperature and it does not include night-time performance.

4.4. Thermal discomfort proportion during heatwave

Proportion in thermal discomfort (TDP) in the building using the eight residential walls during the heatwave period was assessed. TDP is defined as the ratio of number of hours with temperatures exceeding a thermal discomfort threshold to the total hours in a day. The thermal discomfort threshold is chosen as 28 °C according to Chartered Institution of Building Services (CIBSE) Guide A [38]. Table 4 lists the TDP for the eight wall systems and their relative heatwave vulnerability rankings in terms of the TDP index. Achieving the worst comfort level from 25th to 31st January, 'wall G' has a mean proportion in discomfort of 31.5% through the above mentioned 7 day period, which is the highest value observed among other walls. During the extreme hot four days starting from 28th to 31st January 2009, 'wall G' experienced percentages of temperature exceeding the threshold as 50%, 50%, 41.6%, 29.2%, respectively. TDP is capable of evaluating the duration of possible overheating problems in a building, during a period of weather extreme event, by counting number of hours exceeding a specific temperature threshold. TDP provides an indicator for assessing thermal comfort among various building wall designs under weather extreme conditions. It is noted that TDP is an index related to high indoor temperatures which are mainly related to daytime thermal performance.

4.5. Statistical maximum air temperature

The entire data set of predicted hourly room temperatures, calculated during the summer period (i.e. 90 days) with heatwave (TMY weather) and non-heatwave periods (2009 weather), was analysed. The histogram frequency distribution of the hourly room temperature data is presented in Figs. 6 and 7. From Figs. 6 and 7, it was found that during non-heatwave period (i.e. entire summer period in TMY), the frequency for temperature exceeding 28 °C for 'walls A, B, D, H' is nearly zero, but frequency of 5% is observed for 'wall G'. During the hot summer in 2009 where heatwave was

Table 4
Summary of the vulnerability index and relative rankings.

Wall type	A	B	C	D	E	F	G	H
T_{MAX} (°C)	27.72	27.96	29.74	27.78	30.65	30.33	30.65	28.67
Ranking	1	3	5	2	7	6	8	4
AMAT (°C)	27.36	27.54	28.42	27.40	29.30	29.09	29.47	27.93
Ranking	1	3	5	2	7	6	8	4
TDP (>28 °C)	0%	0%	20.2%	0%	29.8%	28.6%	31.5%	13.1%
Ranking	1	1*	5	1*	7	6	8	4
SMAT (5%)(°C)	27.72	27.95	29.73	27.78	30.62	30.31	30.58	28.66
Ranking	1	3	5	2	8	6	7	4
MATD (°C)	1.58	2.05	3.89	1.29	4.09	3.78	4.29	2.24
Ranking	2	3	5	1	7	6	8	4
R^2	0.9031	0.9259	0.9628	0.8968	0.9757	0.9738	0.9595	0.9557
Ranking	2	3	5	1	8	6	7	4
ANT (°C)	26.08	26.04	24.86	26.07	25.68	25.72	25.70	25.85
Ranking	8	6	1	7	2	4	3	5

recorded, 'wall A' and 'wall D' show better heat resilience capability compared with other types of walls with less frequencies at the high temperature range. This statistical difference in heat resilient capability may be identified by the average of the top 5% hourly air temperature defined as Statistical Maximum Air Temperature (SMAT) (5%). Table 4 lists the SMAT (5%) for the eight wall systems and their relative heatwave performance rankings in terms of the SMAT (5%). It is obtained from the data set of predicted hourly room temperature throughout the summer of 2009. It is seen that 'walls A and D' rank the top two walling systems, while 'walls E and G' rank as the worst performers in terms of SMAT (5%).

4.6. Correlation of temperature response

Fig. 8 shows the relationship between the mean daily room temperatures and mean outside temperatures throughout the entire summer in 2009. Fig. 9 shows the mean daily temperature variation for 'wall A' and 'wall G' for the entire 2009 summer including the heat wave period. As shown in Fig. 8, the mean daily room temperatures of the buildings correlate well with the mean ambient air temperature. The response of a specific wall system to extreme hot weather could be predicted through the corresponding correlations obtained under non-heatwave periods.

Table 4 also compares the coefficient of determination, R^2, for all wall structures, which is a measure of the goodness of fit between the internal temperature response to the ambient air temperature and the regression line. It was found that different wall systems have different goodness of fit. Small R^2 values indicate that the indoor temperature does not closely follow the movement of ambient temperature. On the other hand, large R^2 values reflect that indoor temperature closely follows the change

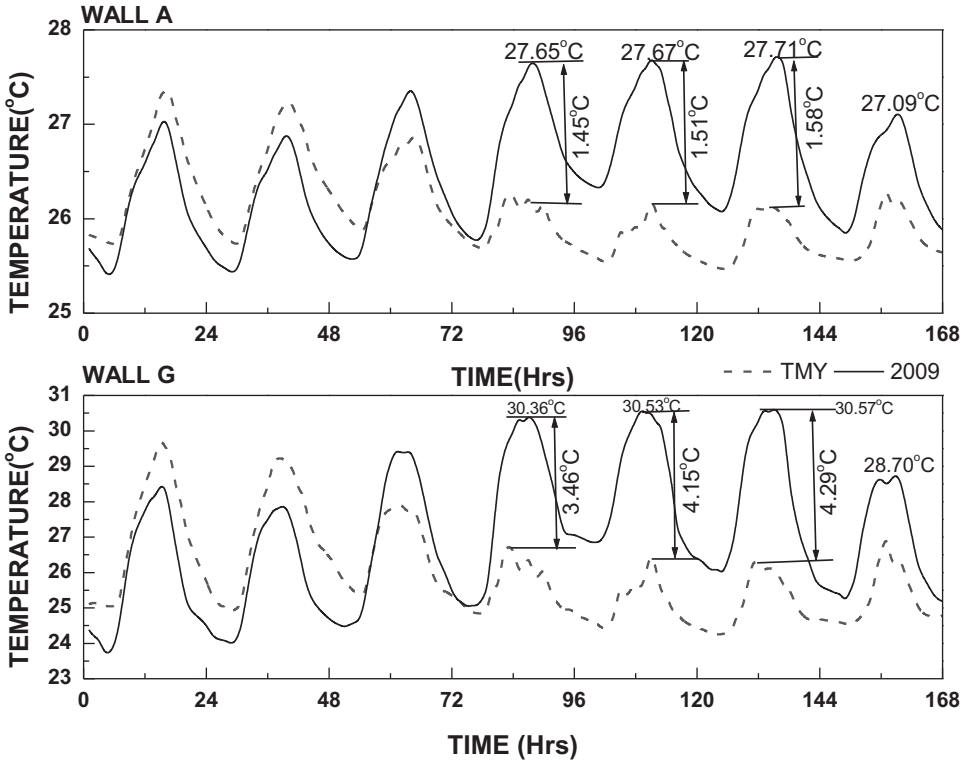

Fig. 5. Room air temperatures for 'wall A' and 'wall G' under TMY and 2009 showing daily maximum air temperature differences (MATD) under two weather conditions for each wall (25th–31st January 2009).

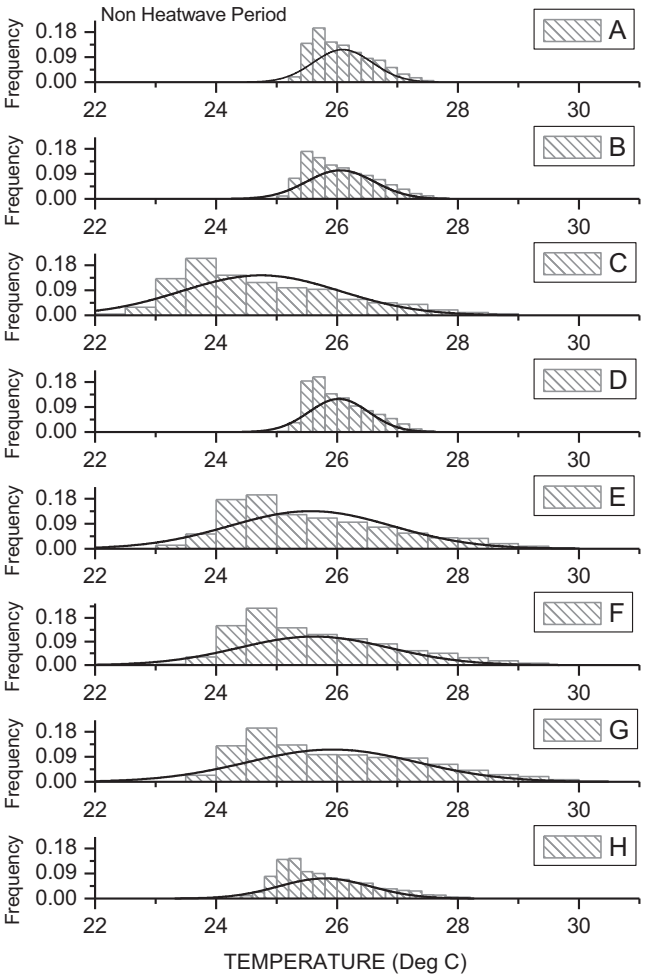

Fig. 6. Histogram of the indoor temperatures for eight typical wall designs in non-heatwave period.

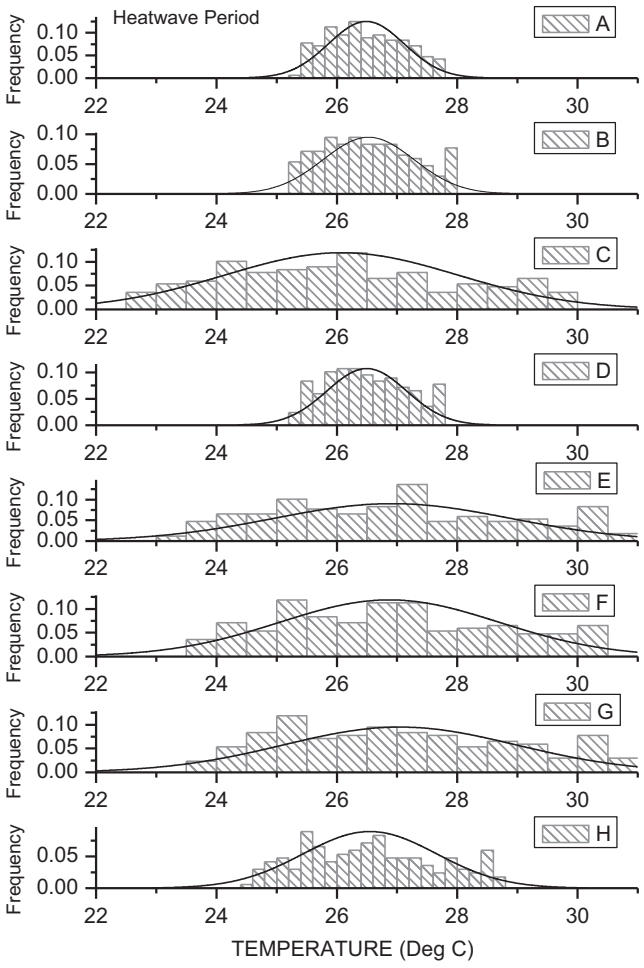

Fig. 7. Histogram of indoor temperatures for eight typical wall designs in heatwave period.

of ambient temperature, and suggest that wall system has less buffering ability to the changes in the ambient weather conditions. As shown in Table 4, 'wall D' is the most resilient design with the lowest R^2 value, $R^2 = 0.90$, while 'wall E' ($R^2 = 0.98$) is most vulnerable to heatwave. We use coefficient of determination, R^2 as the correlation of temperature response (CTR) index. CTR provides an indication of the dynamic relationship between the internal temperatures with outside ambient temperature fluctuations. Using the corresponding correlation, internal temperature could be predicted under given weather conditions, while CTR may provide an index for wall vulnerability assessment.

4.7. Average night-time temperature

Massively constructed wall absorbs heat from sun during daytime and releases it at night, and consequently may result in high room air temperatures during the night in summer period. Because high night temperature constitutes a major factor for health issues and mortality, it is extremely important to consider the thermal comfort at night as well. In order to achieve this goal, an average night-time temperature (ANT) was introduced to compare the night-time thermal performance of each wall from sun set to sun rise. It was found that 'wall C' has a lower ANT of 24.86 °C, while 26.08 °C for 'wall A'. This indicates that additional measures, such as night-time ventilation for removal of absorbed heat, are required to avoid thermal discomfort at night for those walls with better performance at daytime, 'wall A' for example.

4.8. Deviation arising in the above multi-criteria

Moderate or small deviations in the above multi-criteria analysis were observed for daytime thermal performance ranking, as shown in Table 4. According to AMAT, TDP, SMAT, 'wall A' performs better at daytime, while 'wall D' might be a resilient wall system according to MATD. These deviations are due to the different emphasis among these different criteria. However, there is relatively large difference in the ranking between daytime and night-time performance. A wall with good daytime performance has in general a bad night-time performance. 'Wall C' shows a good level of occupant thermal comfort at night-time period. It should be noted that different criteria might be used for houses with different occupant profiles. For example, for occupants who are at home at the daytime during the heatwave period, maximum daily temperature performance may be more important. For house only occupied at night, the night-time performance is critical.

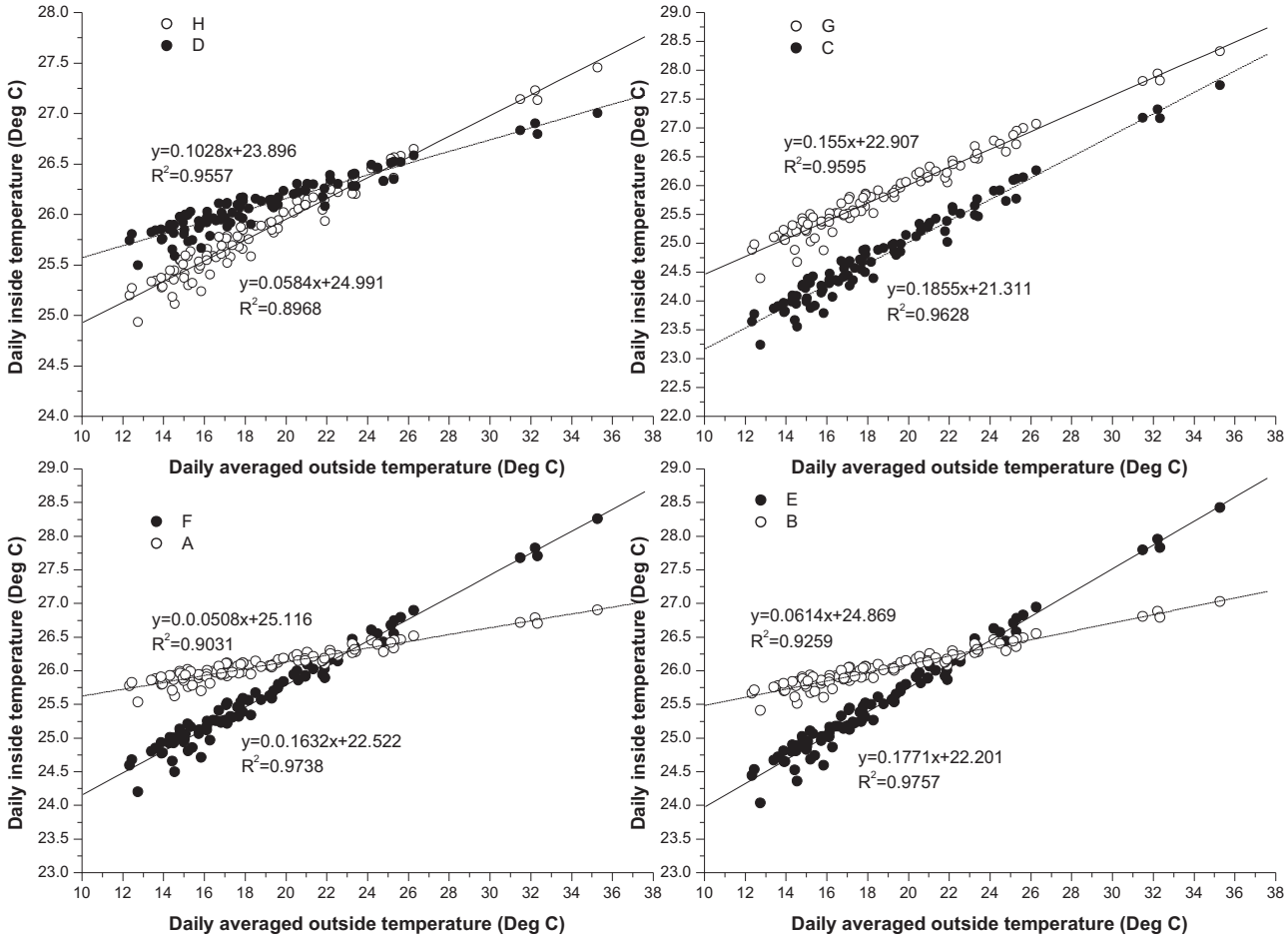

Fig. 8. Scatter plots of internal temperatures against averaged outside temperatures over the summer period from 12/2008 to 02/2009 showing correlation of temperature response (CTR) index for each wall.

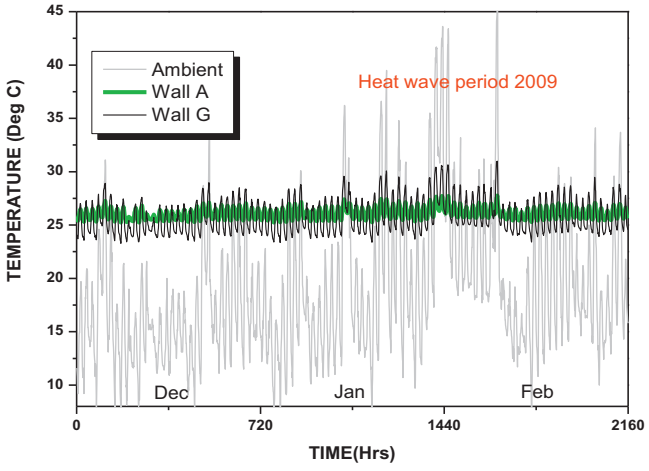

Fig. 9. Room temperature profile for 'wall A' and 'wall G' in summer period.

5. Conclusions

This study provides a dynamic analytical tool to assess heat vulnerability of residential walls for heatwave using a multi-criteria analysis. In order to achieve this goal, a dynamic thermal modelling approach was used to examine the vulnerability of selected Australia residential walls to the heatwave occurred in Melbourne in 2009. The main findings are listed below:

- Although small deviations in ranking exist, the vulnerability rankings for eight selected wall systems are in general consistent when using different vulnerability criteria to evaluate the daytime thermal comfort.
- 'wall G', the popular uninsulated brick veneer wall system, as the most vulnerable wall system among the eight wall systems investigated, results in the largest proportion in discomfort of 31.5% during the heatwave period.
- Using 'wall A', the insulated cavity brick wall, would significantly reduce the discomfort from summer overheating in non-air conditioned buildings in the summer daytime period.
- 'wall A', the insulated cavity brick wall system, as the most resilient design in response to the extreme climate during daytime period, is recommended in Melbourne weather conditions in order to create a thermal comfort environment during heatwave period at daytime. However, night-time ventilation to remove absorbed heat for passively designed building is required to avoid thermal discomfort at night-time.

Further research is needed to identify optimum wall systems in other climates in Australia. Mitigation measures to heatwave through passive building envelope design strategy will also be considered in the future.

Acknowledgements

The authors thank the Department of Climate Change and Energy Efficiency (DCCEE) and the CSIRO Climate Adaptation

Flagship for funding this research. The authors also express their appreciation to Minh N. Nguyen of CSIRO, for valuable advice and generous support.

References

[1] W. Huang, H. Kan, S. Kovats, The impact of the 2003 heat wave on mortality in Shanghai, China, Science of the Total Environment 408 (11) (2010) 2418–2420.
[2] P.A. Stott, D.A. Stone, M.R. Allen, Human contribution to the European heatwave of 2003, Nature 432 (7017) (2004) 610–614.
[3] D. Founda, C. Giannakopoulos, The exceptionally hot summer of 2007 in Athens, Greece — a typical summer in the future climate? Global and Planetary Change 67 (3–4) (2009) 227–236.
[4] D.J. Karoly, The recent bushfires and extreme heat wave in southeast Australia, Bulletin of the Australian Meteorological and Oceanographic Society 22 (2009) 10–13.
[5] State of the Climate: Global Hazards for October 2012, NOAA National Climatic Data Center, 2012.
[6] Climate Change Report Warns of Dramatically Warmer World This Century, The World Bank, 2012.
[7] CSIRO, The science of climate change, 2007.
[8] G.A. Meehl, C. Tebaldi, More intense, more frequent, and longer lasting heat waves in the 21st century, Science 305 (5686) (2004) 994–997.
[9] C. Huang, A.G. Barnett, X. Wang, S. Tong, Effects of extreme temperatures on years of life lost for cardiovascular deaths: a time series study in Brisbane, Australia, Circulation: Cardiovascular Quality and Outcomes 5 (5) (2012) 609–614.
[10] C. Huang, A.G. Barnett, X. Wang, S. Tong, The impact of temperature on years of life lost in Brisbane, Australia, Nature Climate Change 2 (4) (2012) 265–270.
[11] C.B. Huang, A.G. Barnett, X. Wang, P. Vaneckova, G. FitzGerald, S. Tong, Projecting future heat-related mortality under climate change scenarios: a systematic review, Environmental Health Perspectives 119 (12) (2011) 9.
[12] M. Anderson, C. Carmichael, V. Murray, A. Dengel, M. Swainson, Defining indoor heat thresholds for health in the UK, Perspectives in Public Health 133 (3) (2013) 158–164.
[13] B. A.B.C.B., in: C. Australian Building Codes Board (Ed.), The Building Code of Australia, 2009.
[14] A. Roetzel, A. Tsangrassoulis, Impact of climate change on comfort and energy performance in offices, Building and Environment 57 (0) (2012) 349–361.
[15] M.L. Fong, Z. Lin, K.F. Fong, T.T. Chow, T. Yao, Evaluation of thermal comfort conditions in a classroom with three ventilation methods, Indoor Air 21 (3) (2011) 231–239.
[16] W. Liu, Y. Zheng, Q. Deng, L. Yang, Human thermal adaptive behaviour in naturally ventilated offices for different outdoor air temperatures: a case study in Changsha China, Building and Environment 50 (2012) 76–89.
[17] Z. Wang, L. Zhang, J. Zhao, Y. He, Thermal comfort for naturally ventilated residential buildings in Harbin, Energy and Buildings 42 (12) (2010) 2406–2415.
[18] T.G. Nijland, O.C.G. Adan, R.P.J. Van Hees, B.D. Van Etten, Evaluation of the effects of expected climate change on the durability of building materials with suggestions for adaptation, Heron 54 (1) (2009) 37–48.
[19] Z. Ren, Z. Chen, X. Wang, Climate change adaptation pathways for Australian residential buildings, Building and Environment 46 (11) (2011) 2398–2412.
[20] D.P. Jenkins, The importance of office internal heat gains in reducing cooling loads in a changing climate, International Journal of Low-Carbon Technologies 4 (3) (2009) 134–140.
[21] M.R. Gaterell, M.E. McEvoy, The impact of climate change uncertainties on the performance of energy efficiency measures applied to dwellings, Energy and Buildings 37 (9) (2005) 982–995.
[22] C.A. Balaras, The role of thermal mass on the cooling load of buildings. An overview of computational methods, Energy and Buildings 24 (1) (1996) 1–10.
[23] S. Porritt, L. Shao, P. Cropper, C. Goodier, Adapting dwellings for heat waves, Sustainable Cities and Society 1 (2) (2011) 81–90.
[24] S.M. Porritt, P.C. Cropper, L. Shao, C.I. Goodier, Ranking of interventions to reduce dwelling overheating during heat waves, Energy and Buildings 55 (0) (2012) 16–27.
[25] C. Demanuele, A. Mavrogianni, M. Davies, M. Kolokotroni, Using localised weather files to assess overheating in naturally ventilated offices within London's urban heat island, Building Services Engineering Research and Technology 33 (4) (2012) 351–369.
[26] E. Oikonomou, M. Davies, A. Mavrogianni, P. Biddulph, P. Wilkinson, M. Kolokotroni, Modelling the relative importance of the urban heat island and the thermal quality of dwellings for overheating in London, Building and Environment 57 (0) (2012) 223–238.
[27] D.P. Jenkins, M. Gul, S. Patidar, P.F.G. Banfill, G. Gibson, G. Menzies, Designing a methodology for integrating industry practice into a probabilistic overheating tool for future building performance, Energy and Buildings 54 (2012) 73–80.
[28] F. Nicol, M. Humphreys, Maximum temperatures in European office buildings to avoid heat discomfort, Solar Energy 81 (3) (2007) 295–304.
[29] J.F. Nicol, J. Hacker, B. Spires, H. Davies, Suggestion for new approach to overheating diagnostics, Building Research and Information 37 (4) (2009) 348–357.
[30] A. Wright, A. Young, S. Natarajan, Dwelling temperatures and comfort during the August 2003 heat wave, Building Services Engineering Research and Technology 26 (4) (2005) 285–300.
[31] A. Sakka, M. Santamouris, I. Livada, F. Nicol, M. Wilson, On the thermal performance of low income housing during heat waves, Energy and Buildings 49 (2012) 69–77.
[32] ASHRAE, ASHRAE Handbook: Fundamentals (I-P Edition), American Society of Heating, Refrigerating and Air-Conditioning Engineers, Inc., Atlanta, 2009.
[33] J.L. Threlkeld, Thermal Environmental Engineering, Prentice-Hall, 1970.
[34] J. Han, L. Lu, H. Yang, Investigation on the thermal performance of different lightweight roofing structures and its effect on space cooling load, Applied Thermal Engineering 29 (11–12) (2009) 2491–2499.
[35] M. Yazdanian, J.H. Klems, Measurement of the exterior convective film coefficient for windows in low-rise buildings, ASHRAE Transactions 100 (1) (1994) 1087–1096.
[36] GANA, Specifiers Guide to Architectural Glass, 2005 Edition.
[37] R.K. MacGregor, A.F. Emery, Free convection through vertical plane layers—moderate and high Prandtl number fluids, Journal of Heat Transfer 91 (3) (1969) 391–401.
[38] CIBSE, CIBSE Guide A: Environmental Design, Chartered Institution of Building Services Engineers, 2006.
[39] A.M. Coutts, J. Beringer, N.J. Tapper, Investigating the climatic impact of urban planning strategies through the use of regional climate modelling: a case study for Melbourne, Australia, International Journal of Climatology 28 (14) (2008) 1943–1957.